

RECONNECTION RATE IN THE DECAY PHASE OF A LONG DURATION EVENT FLARE ON 1997 MAY 12

HIROAKI ISOBE,^{1,2} TAKAAKI YOKOYAMA,³ MASUMI SHIMOJO,³ TARO MORIMOTO,¹ HIROMICHI KOZU,¹ SHIGERU ETO,^{1,2}
NORIYUKI NARUKAGE,^{1,2} AND KAZUNARI SHIBATA¹

Received 2001 September 25; accepted 2001 October 30

ABSTRACT

Recent analyses of long duration event (LDE) flares indicate successive occurrences of magnetic reconnection and resultant energy release in the decay phase. However, quantitative studies of the energy release rate and the reconnection rate have not yet been made. In this paper we focus on the decay phase of an LDE flare on 1997 May 12 and derive the energy release rate H and the reconnection rate $M_A = v_{\text{in}}/v_A$, where v_{in} is the inflow velocity and v_A is the Alfvén velocity. For this purpose, we utilize a method to determine v_{in} and the coronal magnetic field B_{corona} indirectly, using the following relations:

$$H = 2 \frac{B_{\text{corona}}^2}{4\pi} v_{\text{in}} A_r,$$

$$B_{\text{corona}} v_{\text{in}} = B_{\text{foot}} v_{\text{foot}},$$

where A_r , B_{foot} , and v_{foot} are the area of the reconnection region, the magnetic field strength at the footpoints, and the separation velocity of the footpoints, respectively. Since H , A_r , v_{foot} , and B_{foot} are obtained from the *Yohkoh* Soft X-Ray Telescope data and a photospheric magnetogram, v_{in} and B_{corona} can be determined from these equations. The results are as follows: H is $\sim 10^{27}$ ergs s^{-1} in the decay phase. This is greater than 1/10th of the value found in the rise phase. M_A is 0.001–0.01, which is about 1 order of magnitude smaller than found in previous studies. However, it can be made consistent with the previous studies under the reasonable assumption of a nonunity filling factor. B_{corona} is found to be in the range of 5–9 G, which is consistent with both the potential extrapolation and microwave polarization observed with the Nobeyama Radioheliograph.

Subject headings: Sun: corona — Sun: flares — Sun: X-rays, gamma rays

1. INTRODUCTION

The Soft X-Ray Telescope (SXT; Tsuneta et al. 1991) aboard *Yohkoh* has revealed various new features in solar flares and the corona. One of the most remarkable findings by the *Yohkoh* SXT is the cusp-shaped loop in long duration event (LDE) flares (Tsuneta et al 1992; Hanaoka 1994; Ichimoto et al. 1994; Švestka et al. 1995; Farnik et al. 1996; Tsuneta 1996; Forbes & Acton 1996) and giant arcades associated with filament eruption or coronal mass ejections (CMEs; Hiei, Hundhausen, & Sime 1993; McAllister et al. 1996). Although some previous observations have suggested the presence of the cusp-shaped loops/arcades (MacCombie & Rust 1979; Hanaoka, Kurokawa, & Saito 1986), it was not until after the launch of *Yohkoh* that one began to realize that the cusp structures were common in LDE flares and giant arcades. Since such a cusp structure has been predicted by the standard magnetic reconnection model called the CSHKP model (Carmichel 1964; Sturrock 1966; Hirayama 1974; Kopp & Pneuman 1976), it is considered to be evidence of magnetic reconnection (e.g., Tsuneta 1993; Kosugi & Shibata 1997; Shibata 1996, 1999).

The decay phase of LDE flares is characterized by beautiful cusp-shaped loops/arcades, and hence magnetic recon-

nection is considered to be occurring. On the other hand, the observed cooling times of whole flare loops in the decay phase ($>$ a few hours) is much longer than the theoretical cooling time (~ 1000 s) of each loop due to conduction and radiation. Therefore, there must be significant energy release in the decay phase of LDE flares. It is very likely that such continued energy release is due to successive occurrences of magnetic reconnection (Forbes, Malherbe, & Priest 1989; Hori et al. 1997). In fact, recent analyses of the decay phase of flares support such a reconnection model (e.g., Schmieder et al. 1996; Czaykowska et al. 1999). The physics of the decay phase is, therefore, important in understanding the physics of reconnection. However, no quantitative study has yet been made of the energy release rate and the reconnection rate in the decay phase.

The reconnection rate is defined as the reconnected magnetic flux per unit time or, in dimensionless form, the ratio of the inflow speed (into the reconnection point) to the Alfvén speed. The reconnection rate is one of the most important physical quantities in reconnection physics. A current puzzle in reconnection physics is: what determines the reconnection rate? Sweet (1958) and Parker (1957) predicted that the reconnection rate M_A is as low as $R_m^{-1/2} \sim 10^{-7}$ (n.b., $R_m \sim 10^{14}$ is the magnetic Reynolds number) in the solar corona and thus concluded that reconnection is not important in solar flares, while Petschek (1964) predicted that the reconnection rate is of the order of 0.01–0.1 in the solar corona, which may explain the timescales and energy release rates of solar flares. However, as yet there is no established theory of the physics that determines the

¹ Kwasan and Hida Observatories, Kyoto University, Yamashina, Kyoto 607-8471, Japan; isobe@kwasan.kyoto-u.ac.jp.

² Department of Astronomy, Kyoto University, Kyoto 606-8502, Japan.

³ Nobeyama Radio Observatory, National Astronomical Observatory, Minamisanaka, Nagano 384-1305, Japan.

reconnection rate. Hence, the derivation of the reconnection rate from observations remains important.

A direct observation of the reconnection inflow had not been made until Yokoyama et al. (2001) discovered evidence of an inflow in a limb flare on 1999 May 18. They found the reconnection rate to be 0.001–0.03 in that event. In fact, this is the only example to date of the direct observation of reconnection inflow. Thus, an indirect method is necessary for the derivation of the reconnection rate from observations. Dere (1996) examined the temporal and spatial scales of reconnection events described in the scientific literature and found the reconnection rate to be 0.001–0.1. Tsuneta (1996) and Tsuneta et al. (1997) analyzed flares on 1992 February 21 and 1992 January 13, respectively, and found a rate of 0.06–0.07 for these cases. Ohya & Shibata (1997, 1998) derived the reconnection rate for the impulsive flares (1992 October 5 and 1993 November 11) and found values of 0.0002–0.02 from the preflare to the decay phase.

In the present paper we derive the energy release and reconnection rate in the 1997 May 12 flare. Our study is unique on two points. First, we focus on the decay phase and investigate the temporal variation of the energy release rate and the reconnection rate. Second, we present a method to derive the reconnection rate from observational data with fewer assumptions than in previous studies. The coronal magnetic field strength is also determined by this method. In order to examine the reliability of the analysis, the coronal magnetic field is also estimated by both potential field extrapolation and observation of microwave polarization.

In § 2 we explain the observing methods, and in § 3 we derive the physical parameters of the flare. The methods and results of the derivation of the energy release rate and the reconnection rate are described in § 4. In § 5 the coronal magnetic field is estimated by other methods, and we

compare the results with the value derived in § 4. In § 6 we summarize and discuss our results.

2. OBSERVATIONS

The 1997 May 12 flare is a typical LDE and shows a clear cusp-shaped arcade in *Yohkoh* SXT soft X-ray images (e.g., Sterling et al. 2000). In H α , the Hida Observatory Flare-Monitoring Telescope (FMT) clearly observed two ribbons and a filament eruption (Morimoto et al. 2001, in preparation). An EIT wave and halo CME were also observed by the *SOHO* EUV Imaging Telescope (EIT) and Large Angle Spectrometric and Coronagraph Experiment (LASCO; e.g., Thompson et al. 1998, Plunkett et al. 1998). To derive the energy release rate and reconnection rate we used the *Yohkoh* SXT data and photospheric magnetogram data taken with the *SOHO* Michelson-Doppler Imager (MDI; Scherrer et al. 1995). The SXT data were obtained with the thin aluminum filter (Al.1) or the AlMgMn-sandwich filter (AlMg). We made use of the partial frame images (PFIs) for 05:33:06–06:58:52 and also the full frame images (FFIs) for 08:50:28–15:53:54. The FFI data were used because the PFI field of view does not cover a part of the flare arcade in the late decay phase.

Figure 1 shows the X-ray emission as recorded by the *GOES* 1–8 Å channel (*top curve*) and 0.5–4.0 Å channel (*lower curve*). The shaded areas are *Yohkoh* nights; unfortunately there is no SXT data in the rise phase. The behavior of the X-ray flux is that of a typical LDE flare, i.e., a short (~ 1000 s) rise and a long ($>$ a few hours) decay. Figure 2a shows the SXT images of the preflare phase, and Figures 2b–2f show the decay phase. The observation times of the images are illustrated by the vertical lines in Figure 1. The horizontal and vertical axes give the distance from the disk center in arcseconds. North is up and east is to the left.

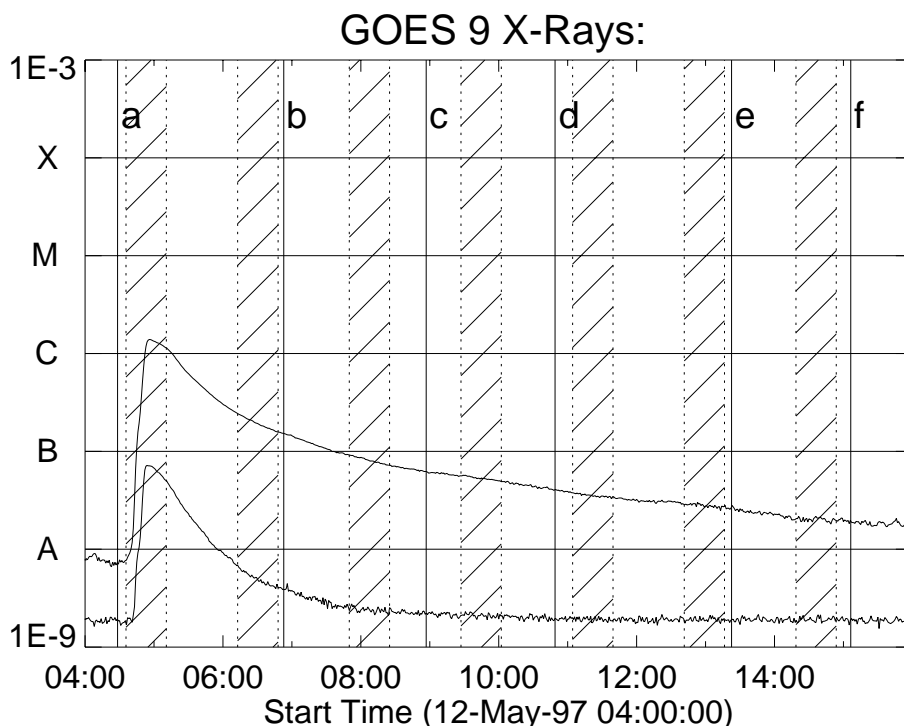


FIG. 1.—X-ray emission as recorded by the *GOES* 1–8 Å channel (*top curve*) and the 0.5–4.0 Å channel (*lower curve*). *Yohkoh* nights and the observation times of the SXT images in Fig. 2 are illustrated by the shaded areas and the vertical lines, respectively.

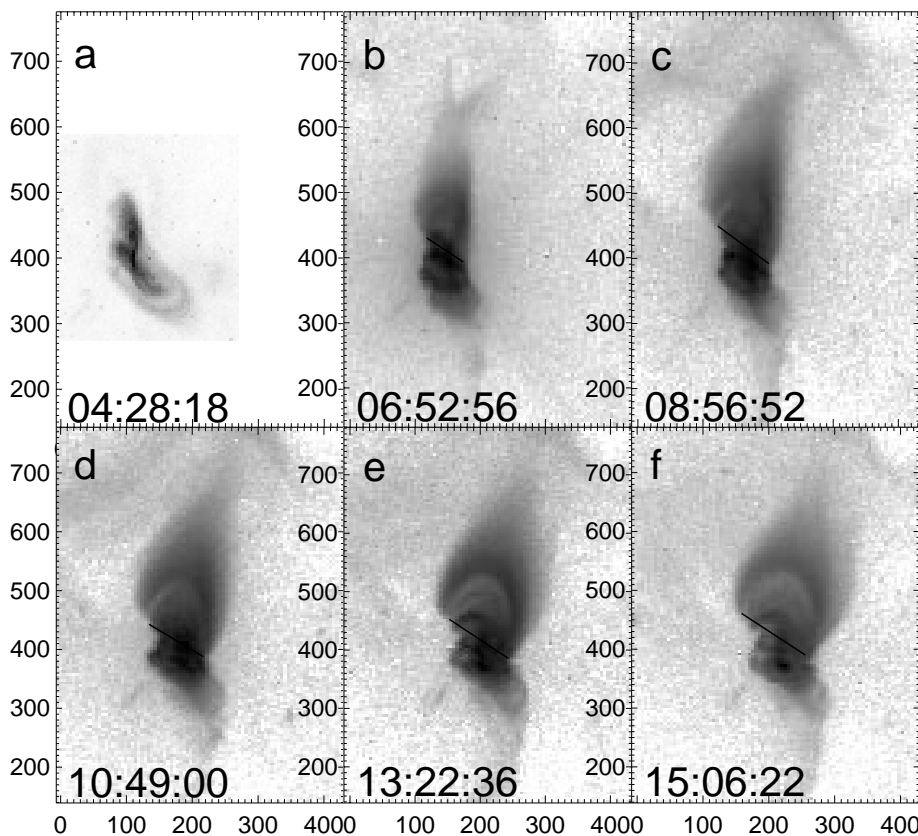


FIG. 2.—SXT images of the LDE flare on 1997 May 12. Panel *a* shows the preflare phase and panels *b–f* show the decay phase. The horizontal and vertical axes give the distance from the disk center in arcseconds. North is up, and east is to the left. The solid lines illustrate the length measured as the distance between the footpoints of the arcade.

Clear cusp-shaped loops are seen at the north and south sides of the flare arcade. The brightest region between the north and south cusp does not show a cusplike structure, probably because of projection effects. Note that the flare arcade continues to evolve even in the late decay phase. This is morphological evidence of ongoing reconnection.

We also made use of microwave images taken with the Nobeyama Radioheliograph (NoRH; Nakajima et al. 1994) to estimate the coronal magnetic field. Figure 3 shows the brightness temperature map of the microwave image obtained with NoRH at a frequency of 17 GHz (*gray scale*). The contours show the SXT image; contour levels are 50, 60, 70, 80, and 90 percent of the maximum intensity. Spectral analysis of the microwave images indicates thermal and optically thin emission, so the coronal magnetic field strength can be estimated by measuring circular polarization. The estimation of the coronal magnetic field from NoRH data is described in § 5.

3. PHYSICAL CONDITIONS

In this section we derive the physical parameters of the flare arcade from the SXT data. In the following analysis, we consider the mean values of the physical parameters in the flare arcade and neglect the spatial structure except for the size and separation velocity of the footpoints.

The temperature T and the volume emission measure EM are derived using the filter ratio method (Hara et al. 1992). Since in many FFIs the flare arcade is saturated and the time cadence of FFI observations with reasonable exposure times is not good, we determined T and EM as follows:

(1) we selected an Al.1 (AlMg) image (obtained at $t = t_0$); (2) we selected two AlMg (Al.1) images with reasonable exposures obtained before ($t = t_1 < t_0$) and after ($t = t_2 > t_0$) the first image; (3) we integrated the intensity of the flare arcade; (4) we derived two temperatures (T_1, T_2) and emission measures (EM_1, EM_2) from the integrated intensities of the two pairs of Al.1 and AlMg images. Finally, we obtained T and EM at $t = t_0$ by linear interpolation, i.e.,

$$T = \frac{T_2 - T_1}{t_2 - t_1} (t_0 - t_1) + T_1. \quad (1)$$

The electron number density n and the thermal energy E_{th} were also calculated, viz.,

$$n = \sqrt{\frac{EM}{V}}, \quad (2)$$

$$E_{\text{th}} = 3nk_B TV, \quad (3)$$

where the volume of the flare arcade V is given by the area on the image A times the line-of-sight length l . In our analysis we assumed that the line-of-sight length was equal to the distance between the footpoints of the arcade. This assumption is justified since we empirically know that the height and the distance between the footpoints of a flare loop are comparable. We also assumed a plasma filling factor of unity. Since Figure 2 shows that the arcade is not uniformly filled with plasma, this estimate gives an upper limit of the volume of the plasma. In the Appendix we discuss how the uncertainty of the volume estimate by these assumptions affects the determination of the energy release

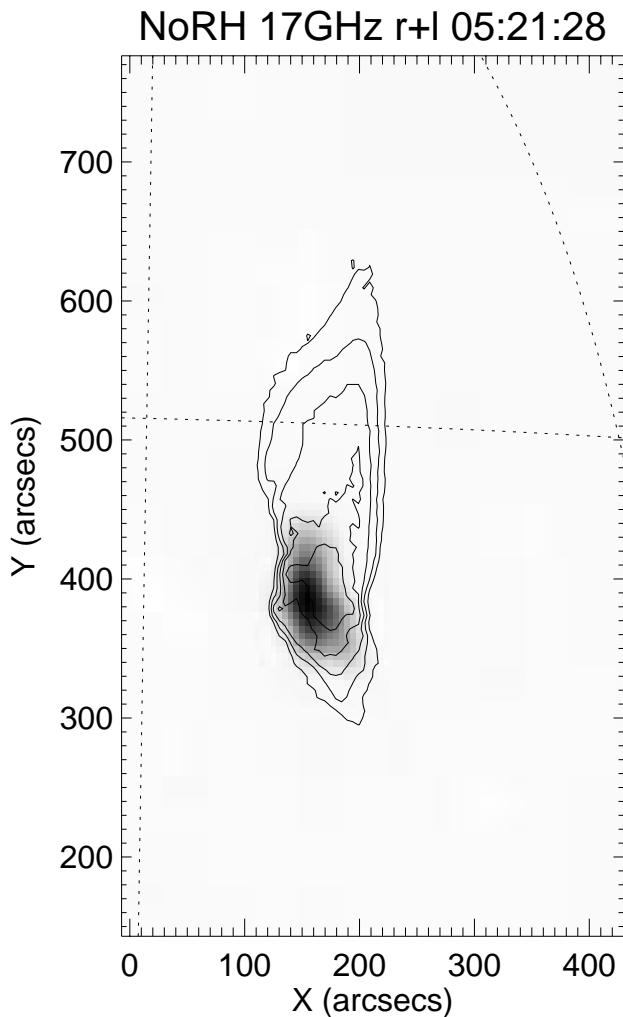


FIG. 3.—Brightness temperature of the microwave image at 17 GHz taken with the NoRH (gray scale) overlaid on the SXT image (contour). The contour levels of the SXT image are 50, 60, 70, 80, and 90 percent of the maximum intensity. The field of view is the same as that of Fig. 2.

rate and the reconnection rate. The measured distances between the footpoints are illustrated by solid lines in Figure 2, and its temporal variation is shown in Figure 4.

Figure 5 shows the temporal variation of the thermal energy, temperature, emission measure, and density. Since

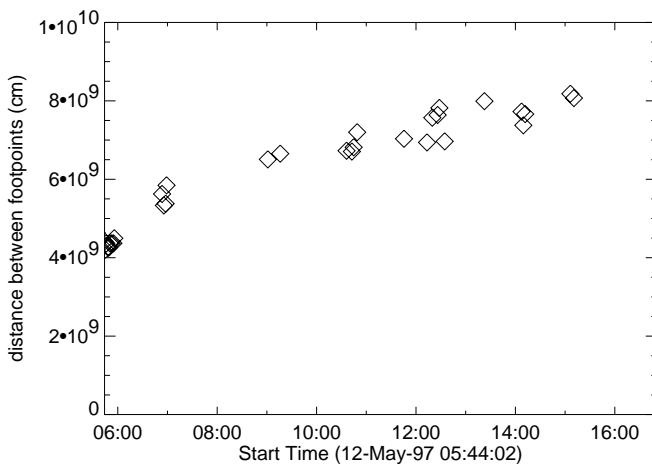


FIG. 4.—Temporal variation of the distance between the footpoints

there is no SXT data for the rise phase, the graphs include only the decay phase. The peak time of *GOES* X-ray flux is about 05:00. The error bars correspond to the two temperatures (T_1 and T_2) and emission measures (EM_1 and EM_2) determined by the method described above, and the diamonds show interpolated values. The time profile of the temperature shows gradual decrease throughout the decay phase from 5 MK to 3 MK, while the emission measure and the electron density decrease rapidly in the early decay phase and gradually in the late decay phase. The decrease of the thermal energy is also very gradual in the late decay phase, indicating ongoing energy release.

4. ENERGY RELEASE RATE AND RECONNECTION RATE

4.1. Energy Release Rate

The energy release rate is defined as the released energy per unit time. For simplicity we assume that all the released energy is converted to thermal energy in the coronal plasma. Since the thermal energy content of the hot plasma in the flare loops depends on the balance between energy input and radiative and conductive losses, the energy release rate H is given by

$$H = \frac{dE_{\text{th}}}{dt} + L_r + L_c. \quad (4)$$

L_r and L_c are the radiative and conductive loss rates, respectively, and are given as follows:

$$L_r = n^2 Q(T) V \approx 10^{-17.73} T^{-2/3} n^2 V \quad (\text{ergs s}^{-1}), \quad (5)$$

$$L_c = \frac{d}{ds} \left(\kappa \frac{d}{ds} T \right) V \approx 9.0 \times 10^{-7} \frac{T^{7/2}}{s^2} V \quad (\text{ergs s}^{-1}), \quad (6)$$

where $Q(T)$ is the radiative loss function for the temperature range $10^{6.3} < T < 10^7$ (Rosner, Tucker, & Vaiana 1978), $\kappa = 9.0 \times 10^{-7} T^{5/2}$ is the Spitzer thermal conductivity (Spitzer 1956), and s is the half-length of the flare loop. Since E_{th} has been obtained as a function of time in § 3, the mean value of dE_{th}/dt can be calculated by least-square fitting. We divided the decay phase into six periods and calculated dE_{th}/dt , L_r , and L_c from the mean values of the parameters in each period. The periods and the mean values of the parameters are summarized in Table 1. Time profiles of H , dE_{th}/dt , L_r , and L_c are shown in Figure 6. The energy release rate is $\sim 10^{27}$ ergs s^{-1} throughout the decay phase, although it decreases slightly.

In the above analysis other energy components, for example, those due to nonthermal particles or lower temperature plasma, were not taken into account. In this sense our estimation of H may be an underestimate. Recent work by Czaykowska, Alexander, & De Pontieu (2001) suggests that any nonthermal component is negligible in the decay phase when compared to thermal conduction, even if chromospheric evaporation is continuously occurring. Lower temperature components can be neglected if the released energy is not directly converted to thermal energy in lower temperature plasma ($T < 2$ MK), which is not seen in the SXT images. On the other hand, the assumption of a filling factor of unity leads to an overestimate of H and may cancel the underestimate; see the Appendix. A detailed analysis of the energy balance of solar flares is required to improve the accuracy of this method.

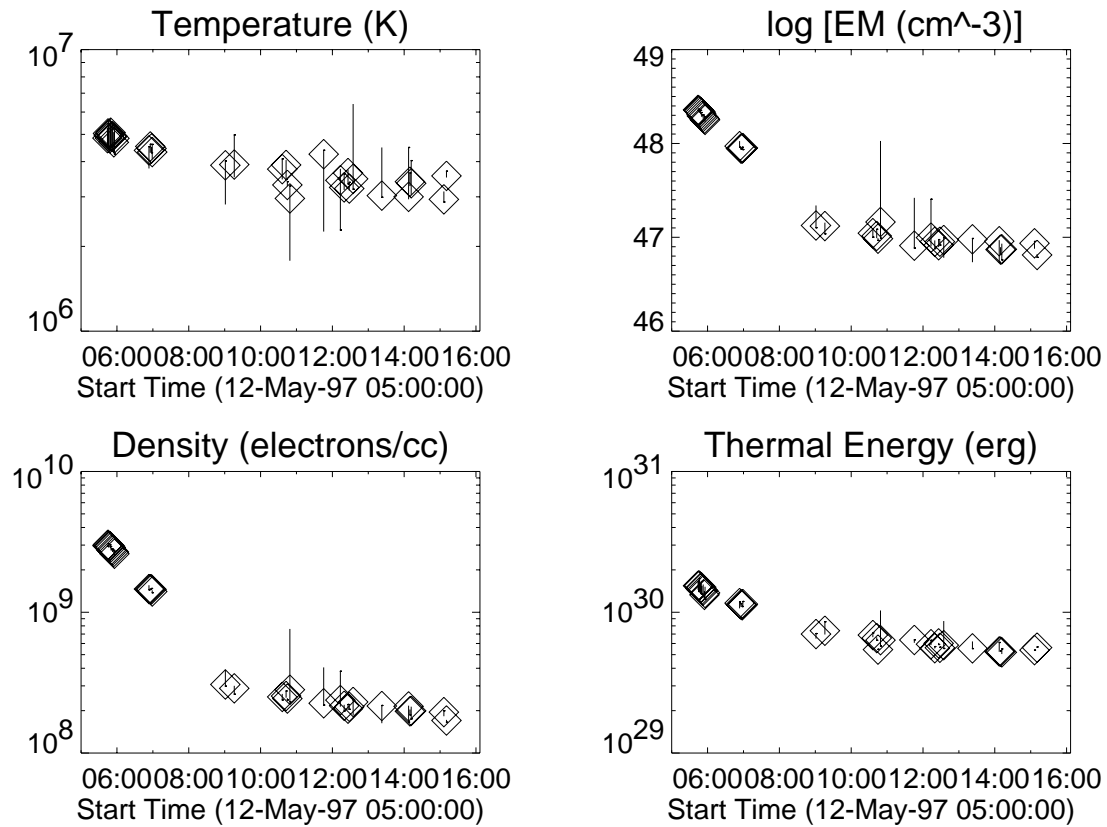


FIG. 5.—Time profiles of temperature, emission measure, density, and thermal energy. The peak time of the X-ray flux is about 05:00.

4.2. Reconnection Rate

The reconnection rate M_A is defined as the ratio of the inflow speed into the reconnection point (v_{in}) to the Alfvén velocity (v_A), namely, $M_A = v_{in}/v_A$. It is not straightforward to determine the reconnection rate from observational data because such an inflow has only been observed in the 1999 March 18 flare by Yokoyama et al. (2001). In this section we utilize an indirect method to determine the reconnection rate from the observational data. A similar method was used by Klimchuk (1996) to estimate the plasma heating rate of an arcade formation event from the photospheric magnetic field. In our approach v_{in} and the coronal magnetic field B_{corona} are simultaneously derived from the SXT data and the MDI photospheric magnetogram.

The released magnetic energy comes from the Poynting flux into the reconnection region so the energy release rate

H is written

$$H = 2 \frac{B_{corona}^2}{4\pi} v_{in} A_r, \quad (7)$$

where A_r is the area of the reconnection region. Since the reconnection region is not directly seen in the SXT image, we assume A_r equals the apparent size of the flare arcade. To obtain the unknown parameters B_{corona} and v_{in} , we use conservation of magnetic flux,

$$B_{corona} v_{in} = B_{foot} v_{foot}. \quad (8)$$

The left-hand side of equation (8) is the reconnected magnetic flux per unit time in the reconnection region, and the right-hand side is the corresponding magnetic flux in the photosphere. As shown in Table 1, v_{foot} is measured as the

TABLE 1
MEAN VALUES OF THE PARAMETERS IN EACH PERIOD.

Parameters	TIME (hr:minutes)					
	05:44–05:56	05:50–06:58	06:53–09:16	09:01–10:49	10:36–12:34	12:13–15:10
T (MK).....	4.9	4.6	4.2	3.5	3.5	3.4
EM ($\times 10^{47} \text{ cm}^{-3}$)	20.4	13.0	4.9	1.3	1.1	0.8
n ($\times 10^8 \text{ cm}^{-3}$)	28.4	20.7	10.7	3.0	2.6	2.1
V ($\times 10^{30} \text{ cm}^3$)	0.25	0.38	0.75	1.6	1.8	2.0
dE_{th}/dt ($\times 10^{26} \text{ ergs s}^{-1}$).....	−3.0	−0.67	−0.53	−0.16	−0.09	−0.05
L_c ($\times 10^{26} \text{ ergs s}^{-1}$)	17.6	10.4	9.1	9.5	8.5	8.2
L_r ($\times 10^{26} \text{ ergs s}^{-1}$)	1.3	0.98	0.62	0.12	0.10	0.07
H ($\times 10^{26} \text{ ergs s}^{-1}$)	16.0	10.7	9.2	9.5	8.5	8.2
v_{foot} (km^{-1}).....	0.86	1.51	0.65	0.27	0.43	0.31

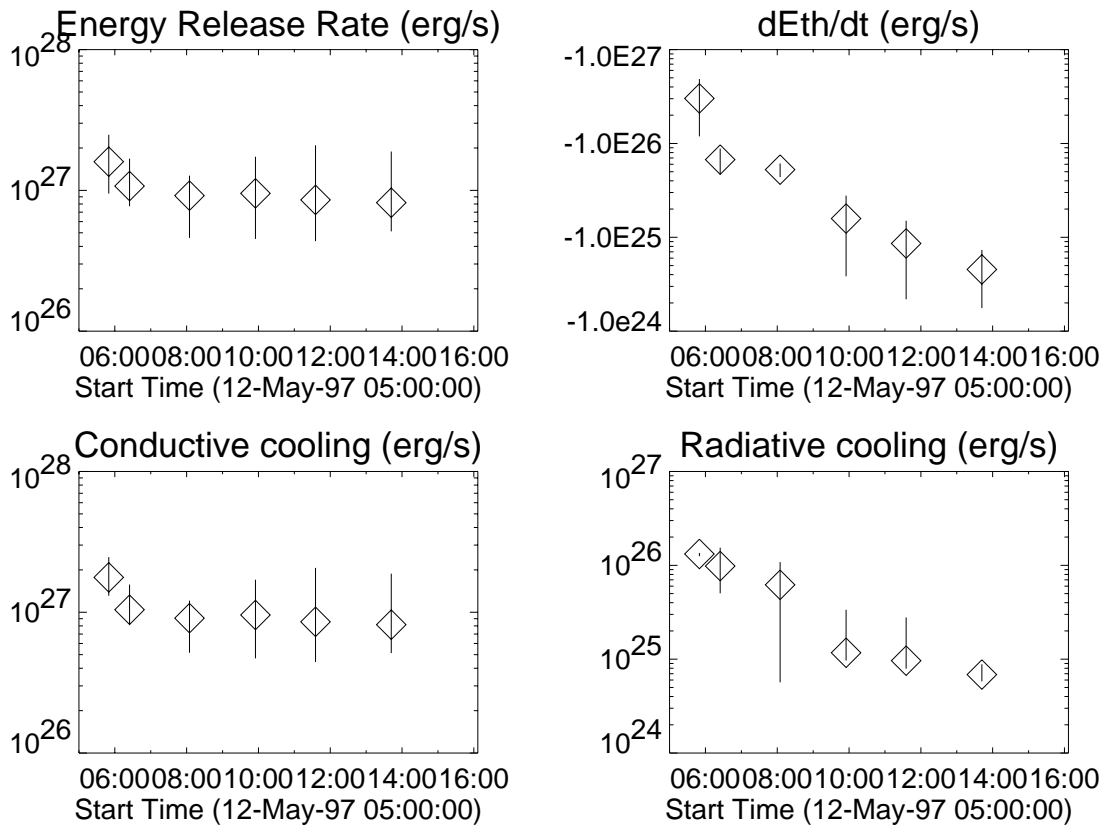


FIG. 6.—Time profiles of the energy release rate, dE_{th}/dt , the radiative cooling, and the conductive cooling. Note that dE_{th}/dt is negative.

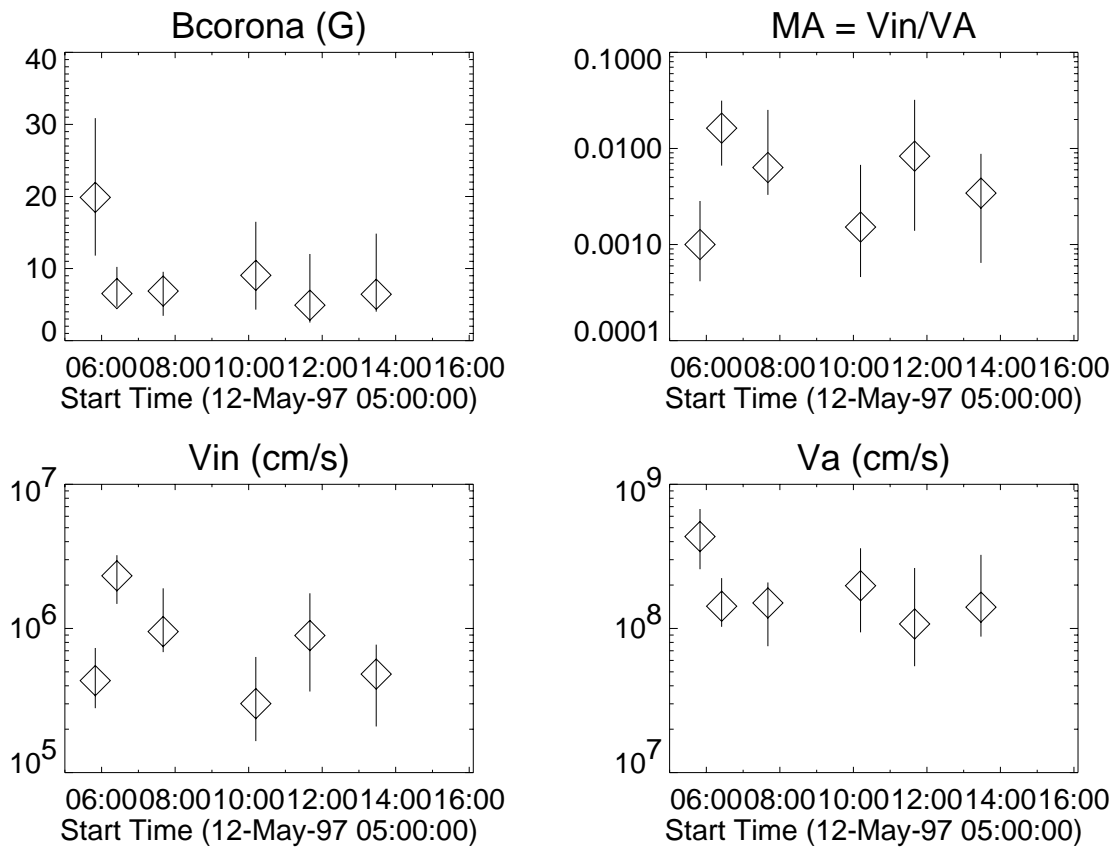


FIG. 7.—Time profiles of B_{corona} , reconnection rate M_A , v_{in} , and v_A

separation velocity of the arcade footpoints. B_{foot} is measured from the photospheric magnetogram. The mean value in the flare arcade region was $B_{\text{foot}} = 100$ G. Thus, the equations (7) and (8) can be solved to obtain B_{corona} and v_{in} .

The Alfvén velocity v_A is expressed as

$$v_A = \frac{B_{\text{corona}}}{\sqrt{4\pi\rho}} = \frac{B_{\text{corona}}}{\sqrt{4\pi n_p m_p}}, \quad (9)$$

where $m_p = 1.67 \times 10^{-24}$ g is the proton mass and n_p is the proton number density (\approx the electron number density n_e) outside the current sheet. The electron number density n_e can be obtained in principle by measuring the EM using the filter ratio method. However, the dark-corrected intensity in the quiet region outside the active region is as low as ~ 20 DN s^{-1} pixel $^{-1}$, and hence the scattered X-ray from the active region is not negligible and must be subtracted using the point spread function (PSF) of SXT. Since the wing component of the PSF is obtained only for the Al.1 filter (Hara et al. 1994), the scattered X-ray can be subtracted only for the Al.1 filter image but not for the AlMg filter image. That is, we cannot use the filter ratio method to derive the temperature and the emission measure. Hence, we assume a temperature to derive the emission measure from the Al.1 filter. Assuming a temperature of 1–3 MK and that the line-of-sight length equals the pressure scale height in the corona, we obtain $n_p \approx n_e = 4 \times 10^7$ – 6×10^8 cm $^{-3}$. We adopted an intermediate value, $n_p = 10^8$ cm $^{-3}$, to calculate v_A and M_A .

Figure 7 shows the temporal variation of B_{corona} , M_A , v_{in} , and v_A . The reconnection rate is 0.001–0.01, which is about 1 order of magnitude smaller than that expected from the fast reconnection model (e.g., Petschek 1964). The coronal magnetic field in the reconnection region is 5–20 G throughout the decay phase. Actually, this method is useful for determining the coronal magnetic field strength in the flare site. In the next section we estimate the coronal magnetic field using other independent methods, and we check the accuracy of our method.

5. CORONAL MAGNETIC FIELD

Our method described in the preceding section can determine B_{corona} and v_{in} simultaneously. Therefore, it can be used to estimate the coronal magnetic field, which is very difficult to measure directly from the observations. In this section we estimate the coronal magnetic field using two other methods: potential field extrapolation and observations of circular polarization of microwave images. We then compare the results with those derived in the previous section.

5.1. Potential Field Extrapolation

A potential field extrapolation has been performed using the Green's function method (Sakurai 1982), and the result is shown in Figure 8. The magnetic field strength in the loop-top region is 3–10 G. Since the actual magnetic field is not likely to be different from the potential field by more than 1 order of magnitude, this is consistent with the results of § 4.

5.2. Microwave Polarization

The coronal magnetic field can be directly derived by measuring circular polarization of microwaves if the plasma is thermal and optically thin. In fact, this is the only method of direct observation of the coronal magnetic field. NoRH is a very powerful instrument for this purpose because a polarization degree of less than 1% is detectable with high spatial resolution.

The degree of circular polarization is defined as

$$r_c = \frac{T_{b,R} - T_{b,L}}{T_{b,R} + T_{b,L}}, \quad (10)$$

where $T_{b,R}$ and $T_{b,L}$ are brightness temperatures for right- and left-handed circular polarization, respectively. For a thermal and optically thin plasma Dulk (1985) gives

$$r_c \approx 2(v_B/v) \cos \theta, \quad (11)$$

where $v_B = eB/(2\pi m_e c)$ is the electron-cyclotron frequency, v is the observing frequency, and θ is the angle between the

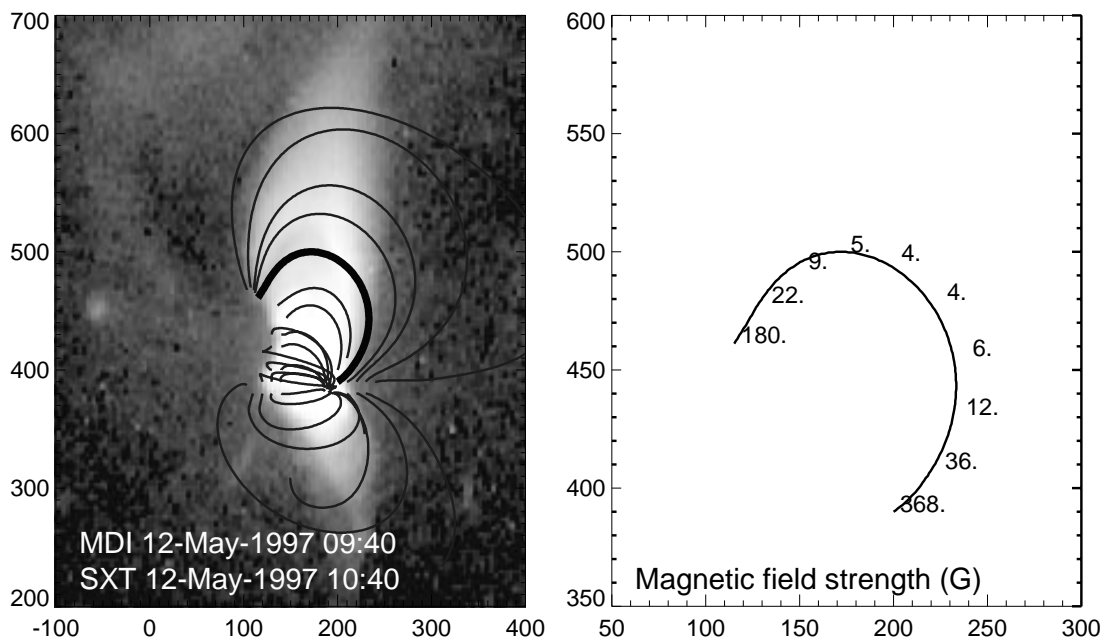


FIG. 8.—Potential field line on SXT image (left panel) and the magnetic field strength along the thick line (right panel)

magnetic field line and the line of sight. Since NoRH observes circular polarization at a frequency of 17 GHz, substituting $\nu = 17 \times 10^9$ Hz in equation (11), we obtain

$$B \cos \theta = \frac{\pi m_e c}{e} \nu r_c \approx 3000 \times r_c. \quad (12)$$

Thus, the line-of-sight component of the magnetic field in the corona can be directly obtained by measuring the circular polarization r_c .

Figure 9 shows the polarization degree overlaid on the photospheric magnetogram (*gray scale*). The polarization degree is shown by the thick contours. Contour levels are -1 , 2 , 3 , and 4 percent, and the red and blue contours correspond to positive and negative values, respectively. The thin contours (*red and blue*) are the photospheric magnetic field. Contour levels are ± 50 , ± 100 , ± 200 , and ± 500 gauss; red is for positive, and blue is for negative. The yellow contours show the brightness temperature of the NoRH 17 GHz image. Contour levels are 2×10^4 , 5×10^4 , and 1×10^5 K. The polarization degree is less than 1% in the top region of the flare arcade, that is, in the brightest region of the NoRH image, so B_{corona} is estimated to be less than 30 G. This is also in agreement with the value derived in § 4

6. DISCUSSION

It is generally believed that continuous magnetic reconnection and the resultant energy release is occurring in the decay phase of LDE flares (e.g., Schmieder et al. 1995, 1966; Harra-Murnion et al. 1998). The main goal of this paper is to derive the energy release rate and the reconnection rate in the decay phase of an LDE flare. For this purpose we have present a new method to derive the reconnection rate and apply it to the decay phase of a flare observed on 1997 May 12 by *Yohkoh* SXT.

We find that the energy release rate is 2×10^{27} ergs s^{-1} near the peak time and that it decreases slightly to 8×10^{26} ergs s^{-1} in the late decay phase. To give an indication of its size, we estimate the energy release rate in the rise phase. Although the rise phase is not covered by the *Yohkoh* observations, the energy release rate can be roughly estimated from the thermal energy of the flare arcade near the peak time and the rise time of the *GOES* X-ray flux. By extrapolating the time profile of thermal energy in Figure 5, the thermal energy near the X-ray peak time (about 05:00) is estimated to be $(2-3) \times 10^{30}$ ergs. On the other hand, the *GOES* X-ray flux shows that the rise time is about 1000 s. Considering the effect of cooling, the energy release rate in the rise phase is $\sim (3-5) \times 10^{27}$ ergs s^{-1} . Thus, the energy

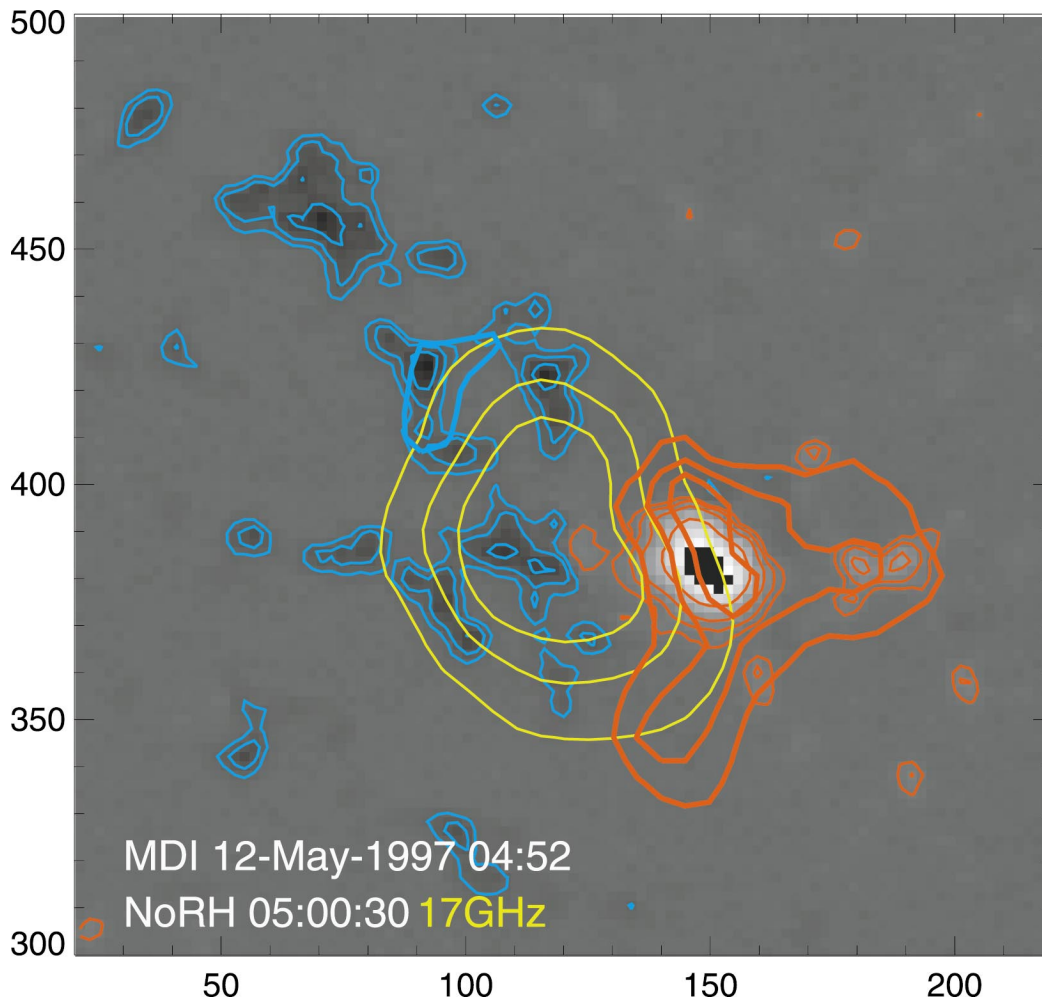


FIG. 9.—Degree of circular polarization (*thick contours*) overlaid on the photospheric magnetogram (*gray scale*). Contour levels of circular polarization are -1 , 2 , 3 , and 4 percent. The thin contours (*red is positive and blue is negative*) are the photospheric magnetic field; contour levels are ± 50 , ± 100 , ± 200 , and ± 500 gauss. The yellow contours show the NoRH 17 GHz image.

TABLE 2
OBSERVATIONAL DERIVATION OF THE RECONNECTION RATE

Author	Reconnection Rate	Event
Dere 1996.....	0.001–0.1	Many events in scientific literature
Tsuneta 1996.....	0.07	1992 Feb 21
Tsuneta et al. 1997.....	0.06	1992 Jan 13
Ohyama & Shibata 1997.....	0.0002–0.13	1993 Nov 11
Ohyama & Shibata 1998.....	0.02	1992 Oct 5
Forbes & Lin 2000.....	0.03	No particular event
Yokoyama et al. 2001.....	0.001–0.03	1999 Mar 18
This paper.....	0.001–0.01	1997 May 12 (decay phase)

release rate in the decay phase is of the order of that in the rise phase.

This energy release is very likely due to ongoing magnetic reconnection. Other possibilities, such as dissipation of the current sheet confined in the flare loops, cannot explain the morphological evolution, i.e., the cusp-shaped arcade and its separating footpoints. In Table 2 we summarize the reconnection rate derived from observation in this paper and the rates derived in previous studies. The results from previous studies are almost consistent with the theoretical prediction, 0.01–0.1, of the fast reconnection model of Petschek (1964). On the other hand, our result is about 1 order of magnitude smaller. In the case of an impulsive flare, Ohyama & Shibata (1997) found that the reconnection rate is smaller in the decay phase than in the impulsive phase. Our result indicates that this is also true in LDE flares.

However, the assumption of a plasma filling factor of unity may lead to an underestimate of the reconnection rate, and thus the derived reconnection rate is a lower limit. Let f and f_r denote the plasma filling factor in the flare arcade and in the reconnection region, respectively. For $f = 0.1$ and $f_r = 0.3$, the reconnection rate M_A increases to 0.01–0.1, which is in line with the previous results. The effect of the filling factors on the calculated reconnection rate is discussed in the Appendix.

Finally, we remark on the other methods of observational derivation of the reconnection rate. As mentioned in § 4, the reconnection inflow has not been observed except in the EIT observations of Yokoyama et al. (2001). Indirect derivation of the reconnection rate is therefore necessary for the study of magnetic reconnection. Dere (1996) examined the timescale τ and the spatial scale L of reconnection events in the solar corona described in the scientific literature and found L/τ to be $0.01\text{--}0.1v_A$ for these events. His study is significant because many events are examined statistically. However, as he pointed out, he did not derive the speed of the reconnection process itself, but the speed of the geometric change of the magnetic field configuration. Tsuneta (1996) derived the reconnection rate for an LDE flare by estimating the half-angle of slow shocks from SXT images. This method assumes the Petschek-type reconnection model. Tsuneta et al. (1997) and Ohyama & Shibata (1997, 1998) also used the SXT data and considered equa-

tion (7). To obtain B_{corona} and v_{in} , they assumed the following pressure balance:

$$P_{\text{in}} = P_{\text{out}} + \frac{B_{\text{corona}}^2}{8\pi}, \quad (13)$$

where P_{in} and P_{out} are the gas pressure inside and outside the current sheet, respectively. If one assumes that P_{in} and P_{out} are comparable to the gas pressures inside and outside the flare loop, respectively, they can be estimated from the SXT data, so that B_{corona} and v_{in} are derived from equations (7) and (13). More recently Forbes & Lin (2000) have presented a method to determine the reconnection rate from CME observations. They chose some typical values for observational quantities and determined $M_A = 0.03$. Their method, however, requires a model of the coronal magnetic field and the coronal density.

The method presented in this paper is an extension of the methods developed by Tsuneta et al. (1997) and Ohyama & Shibata (1997, 1998). The main differences are the use of the photospheric magnetogram and equation (8), which allow us to derive the reconnection rate without the assumption of equation (13) or any assumption about the reconnection model. Another advantage of our method is that it can be used to determine the coronal magnetic field strength, particularly in flares or giant arcade formations. This method can be applied to many events, provided the SXT data and the photospheric magnetogram are available. A statistical study of the reconnection rate using this method will provide us with much more information on the reconnection model.

The authors thank K. Shibasaki and D. Brooks for carefully reading the manuscript and helpful comments. The calculation of the potential field was performed using the software package developed by T. Sakurai. The *Yohkoh* satellite is a Japanese national project, launched and operated by ISAS, and involving many domestic institutions, with multilateral international collaboration with the US and the UK. *SOHO* is a mission of international cooperation between the European Space Agency (ESA) and NASA.

APPENDIX A

EFFECT OF THE FILLING FACTOR AND LINE-OF-SIGHT LENGTH

In order to determine the energy release rate, we assumed a plasma filling factor f of unity and that the line-of-sight length l equals the distance between the arcade footpoints that can be measured from the SXT images. Since the volume of the plasma

is given by $V = Alf$, the electron density n and thermal energy E_{th} are written as

$$n = \sqrt{\frac{EM}{V}} \propto (lf)^{-1/2}, \quad (\text{A1})$$

$$E_{\text{th}} = 3nk_{\text{B}}TV \propto (lf)^{1/2}. \quad (\text{A2})$$

The radiative loss rate L_r is given by

$$L_r = n^2Q(T)V = EMQ(T) \propto (lf)^0. \quad (\text{A3})$$

L_r is independent of the volume estimation. The conductive loss rate L_c is given by

$$L_c = \frac{\kappa_0 T^{7/2}}{s^2} V \propto (lf)^1. \quad (\text{A4})$$

In § 4.1 we see that the conductive loss ($\sim 10^{27}$ ergs s^{-1}) is dominant compared to the other terms in equation (4) ($\sim 10^{25-26}$ ergs s^{-1}). Hence, H is roughly proportional to $(lf)^1$;

$$H = \frac{dE_{\text{th}}}{dt} + L_r + L_c \propto (lf)^1. \quad (\text{A5})$$

Equation (A5) shows the dependence of the energy release rate on the plasma filling factor and the line-of-sight length. Since we empirically know that the height and the distance between the footpoints of a flare loop are nearly equal, the uncertainty of l is likely to be less than a factor of 2. Takahashi (1997) estimated the filling factor in 59 flares and found $f = 0.1-1$. If $f = 0.1$, the conductive loss and the radiative loss become comparable, and the energy release rate is reduced by an order of magnitude.

An alternative method to avoid the uncertainty of the volume estimate is that of Doyle & Raymond (1984), who adopted the density n as a parameter rather than the volume to determine the energy release rate and measured n independently by spectroscopy. Their method is useful if n can be determined independently, although it is not enough to determine the reconnection rate.

In order to determine the reconnection rate M_A we need to estimate the area of reconnection region A_r . Here we also consider the filling factor of the reconnection inflow f_r . Then equation (7) is written as

$$H = 2 \frac{B_{\text{corona}}^2}{4\pi} v_{\text{in}} A_r f_r. \quad (\text{A6})$$

Taking into account $H \propto (lf)^1$, B_{corona} , v_{in} , and M_A are given by

$$B_{\text{corona}} = \frac{2\pi H}{B_{\text{foot}} v_{\text{foot}} A_r f_r} \propto A_r^{-1} l^1 \left(\frac{f}{f_r}\right)^1, \quad (\text{A7})$$

$$v_{\text{in}} = \frac{(B_{\text{foot}} v_{\text{foot}})^2 A_r f_r}{2\pi H} \propto A_r^1 l^{-1} \left(\frac{f}{f_r}\right)^{-1}, \quad (\text{A8})$$

$$M_A = \frac{v_{\text{in}}}{B_{\text{corona}}/\sqrt{4\pi\rho}} \propto A_r^2 l^{-2} \left(\frac{f}{f_r}\right)^{-2}. \quad (\text{A9})$$

Here we neglect the filling factor dependence of $\sqrt{\rho} \propto f_r^{1/4}$, which is relatively small because of the square root. Equations (A7), (A8), and (A9) show that the assumption of a filling factor f of unity gives an upper limit of B_{corona} and lower limits of v_{in} and M_A . The reconnection rate derived with an assumption of $f = f_r = 1$ in § 4 is $M_A \approx 0.001-0.01$. For $f_r = 0.3$ and $f = 0.1$ M_A increases to 0.01–0.1. This value of M_A is comparable to the previous results (Dere 1996; Tsuneta 1996; Tsuneta et al. 1997; Ohyama & Shibata 1997, 1998; Forbes & Lin 2000; Yokoyama et al. 2001). For $f_r = 1$ and $f = 0.1$ M_A increase to 0.1–1, which seems to be unrealistically large. If the filling factor is the same in the flare arcade and in the reconnection region, that is, if $f/f_r = 1$, the dependence of the filling factor of the derived B_{corona} , v_{in} , and M_A vanishes.

REFERENCES

- Carmichael, H. 1964, in *The Physics of Solar Flares*, ed. W. N. Hess (NASA SP-50), 451
- Czaykowska, A., Alexander, D., & De Pontieu, B. 2001, *ApJ*, 552, 849
- Czaykowska, A., De Pontieu, B., Alexander, D., & Rank, G. 1999, *ApJ*, 521, L75
- Dere, K. P. 1996, *ApJ*, 472, 864
- Doyle, J. G., & Raymond, J. C. 1984, *Sol. Phys.*, 90, 97
- Dulk, G. A. 1985, *ARA&A*, 23, 169
- Farnik, F., Svestka, Z., Hudson, H. S., & Uchida, Y. 1996, *Sol. Phys.*, 168, 331
- Forbes, T. G., & Acton, L. W. 1996, *ApJ*, 459, 330
- Forbes, T. G., & Lin, J. 2000, *J. Atmos. Sol.-Terr. Phys.*, 62, 1499
- Forbes, T. G., Malherbe, J. M., & Priest, E. R. 1989, *Sol. Phys.*, 120, 285
- Hanaoka, Y. 1994, in *Proc. Kofu Symp.*, ed. S. Enome, & T. Hirayama, NRO Report 360 (Nagano: Nobeyama Radio Obs.), 181
- Hanaoka, Y., Kurokawa, H., & Saito, S. 1986, *Sol. Phys.*, 105, 133
- Hara, H., Tsuneta, S., Acton, L. W., Bruner, M. E., Lemen, J. R., & Ogawara, Y. 1994, *PASJ*, 46, 493
- Hara, H., Tsuneta, S., Lemen, J. R., Acton, L. W., & McTiernan, J. M. 1992, *PASJ*, 44, L135
- Harra-Murnion, L. K., et al. 1998, *A&A*, 337, 911
- Hiei, E., Hundhausen, A., & Sime, D. G. 1993, *Geophys. Res. Lett.*, 20, 2785
- Hirayama, T. 1974, *Sol. Phys.*, 34, 323
- Hori, K., Yokoyama, T., Kosugi, T., & Shibata, K. 1997, *ApJ*, 489, 426
- Ichimoto, K., et al. 1994, in *X-Ray Solar Physics from Yohkoh*, ed. Y. Uchida, et al. (Tokyo: Universal Academy Press), 259
- Klimchuk, J. A. 1996, in *ASP Conf. Ser. 111, Magnetic Reconnection in the Solar Atmosphere*, ed. R. D. Bentley & J. T. Mariska (San Francisco: ASP), 319
- Kopp, R. A., & Pneuman, G. W. 1976, *Sol. Phys.*, 50, 85

- Kosugi, T., & Shibata, K. 1997, in *Magnetic Storms* (Geophys. Monogr. 98, Washington, DC: AGU), 21
- MacCombie, W. J., & Rust, D. M. 1979, *Sol. Phys.*, 61, 69
- McAllister, A., H., Dryer, M., McIntosh, P., Singer, H., & Weiss, L. 1996, *J. Geophys. Res.*, 101, 13497
- Nakajima, H., et al. 1994, in *Proc. IEEE*, 82, 705
- Ohyama, M., & Shibata, K. 1997, *PASJ*, 49, 249
- . 1998, *ApJ*, 499, 934
- Parker, E. N. 1957, *J. Geophys. Res.*, 62, 509
- Petschek, H. E. 1964, in *AAS-NASA Symp. on Solar Flares*, ed. W. N. Hess (NASA SP-50), 425
- Plunkett, S. P., Thompson, B. J., Howard, R. A., Michels, D. J., St. Cyr, O. C., Tappin, S. J., Schwenn, R., & Lamy, P. L. 1998, *Geophys. Res. Lett.*, 25, 2477
- Rosner, R., Tucker, W. H., & Vaiana, G. S. 1978, *ApJ*, 220, 643
- Sakurai, T. 1982, *Sol. Phys.*, 76, 301
- Schmieder, B., Heinzel, P., van Driel-Geztesy, L., & Lemen, J. R. 1996, *Sol. Phys.*, 165, 303
- Schmieder, B., Heinzel, P., Wiik, J. E., Lemen, J., Anwar, B., Kotrc, P., & Hiei, E. 1995, *Sol. Phys.*, 156, 337
- Sherrer, P. H., et al. 1995, *Sol. Phys.*, 162, 129
- Shibata, K. 1996, *Adv. Space Res.*, 17, (4/5), 9
- . 1999, *Ap&SS*, 264, 129
- Spitzer, L. 1956, *Physics of Fully Ionized Gases* (New York: Interscience)
- Sterling, A. C., Hudson, H. S., Thompson, B. J., & Zarro, D. M. 2000, *ApJ*, 532, 628
- Sturrock, P. A. 1966, *Nature*, 211, 695
- Švestka, Z., Fárnik, F., Hudson, H. S., Uchida, Y., Hick, P., & Lemen, J. R. 1995, *Sol. Phys.*, 161, 331
- Sweet, P. A. 1958, in *IAU Symp. 6, Electromagnetic Phenomena in Cosmical Physics*, ed. B. Lehnert (Cambridge: Cambridge Univ. Press), 123
- Takahashi, M. 1997, Ph.D. thesis, Graduate University for Advanced Studies (Nat'l. Astron. Obs.)
- Thompson, B. J., Plunkett, S. P., Gurman, J. B., Newmark, J. S., St. Cyr, O. C., Michel, D. J., & Delaboudinière, J. -P. 1998, *Geophys. Res. Lett.*, 25, 2461
- Tsuneta, S. 1993, in *Proc. IAU Colloq. 141, Magnetic and Velocity Fields of Solar Active Regions*, ed. H. Zirin, G. Ai, & H. Wang (ASP Conf. Ser. 46; San Francisco: ASP), 239
- . 1996, *ApJ*, 456, 840
- . 1991, *Sol. Phys.*, 136, 37
- Tsuneta, S., Hara, H., Shimizu, T., Acton, L. W., Strong, K. T., Hudson, H. S., & Ogawara, Y. 1992, *PASJ*, 44, L63
- Tsuneta, S., Masuda, S., Kosugi, T., & Sato, J. 1997, *ApJ*, 478, 787
- Yokoyama, T., Akita, K., Morimoto, T., Inoue, K., & Newmark, J. 2001, *ApJ*, 546, L69